DOI: 10.61782/fa.2025.0579

FORUM ACUSTICUM
EURONOISE 2025

MODELLING OF DISTORTIONS CREATED BY TEMPORAL INTERACTIONS BETWEEN PULSES IN CI USERS

François Guérit[1*] **Charlotte Garcia**[1] **Robert P. Carlyon**[1]

[1] Cambridge Hearing Group, MRC Cognition and Brain Sciences Unit, University of Cambridge, United Kingdom

ABSTRACT

With Cochlear Implants (CIs), interleaving two pulse trains modulated respectively at 80 and 120 Hz produces a neural distortion response (NDR) at 40 Hz in the cortical EEG response. Understanding how this NDR is generated may help diagnose the auditory nerve (AN) physiological status of CI users.

We investigated two phenomenological models of the AN, one that included refractoriness and spike-rate adaptation (BR22), and one that additionally included facilitation and accommodation (JO17). The two pulse trains were separated by an inter-pulse interval (IPI) ranging from 0 to 1000 µs. We quantified the summed neural activity at 40 Hz.

Both models created an NDR. At IPIs below 400 µs and in the JO17 model, this was driven by facilitation between pulses, while at IPIs above 400 µs (and all IPIs for the BR22 model), refractoriness was the main generation mechanism. Neither model predicted the reduction in NDR at longer IPIs seen in humans, but a modified version (with a faster release from refractoriness) of the BR22 model could. The phase of the NDR was better predicted by refractoriness generation than facilitation. This suggests NDRs may already be present at the level of the AN and reflect core temporal-interaction mechanisms.

Keywords: *cochlear implants, distortions, modelling, refractoriness, facilitation*

***Corresponding author**: *francois.guerit@mrc-cbu.cam.ac.uk.*

1. INTRODUCTION

Cochlear Implants (CIs) recreate tonotopicity by extracting the speech envelope in different frequency bands and stimulating accordingly different electrodes ('channels') with a rapid succession of electrical pulses [1]. The spiral ganglions forming the auditory nerve (AN) spike in response to such electrical pulses depending on each pulse amplitude/charge, but spiking is also highly dependent upon interactions between pulses. Phenomena such as refractoriness, facilitation, accommodation, and spike-rate adaptation all play a role, each at various timescales [2]. Physiological differences between recipients (and between cochlear locations within participants) are likely to impact temporal interactions between pulses, and thus the encoding of sounds.

We recently developed a method to record electroencephalography (EEG) responses (of cortical/thalamus origin) at high stimulation rates by interleaving two pulse trains (modulated respectively at F1 = 80 and F2 = 120 Hz) and measuring the neural distortion response (NDR) at F2-F1 = 40 Hz [3, 4]. The presence of an NDR means that the effect of interleaving is "undone" by some integration mechanism, prior to a nonlinearity. We argued in [4] that the AN could already be the locus of such integration, because of the temporal interactions described above. For example, increasing the inter-pulse interval (IPI) between the two pulse trains past 400 µs decreased the NDR significantly, while thalamus/cortex is known to have longer time constants of integration [4].

Given the $\sim$ 400 µs time constant seen in [4], two mechanisms are most likely to be involved: refractoriness and/or facilitation. Absolute refractoriness is when a neuron cannot physically spike again for a few hundred microseconds after spiking once. It is followed by a period

of relative refractoriness (elevated thresholds) that can last up to a few milliseconds. Facilitation is when two subthreshold pulses are enough to generate a spike, if presented within a few hundred microseconds. To disentangle such effects, we investigated two models of the AN, one that included refractoriness (BR22, [5]), and one that additionally included facilitation (JO17, [6]). [1]

2. METHODS

BR22 model. The model consists of 1500 neurons distributed along the cochlea. For each combination of stimulating electrode and neuron, a look-up table gives the threshold of spiking (obtained with single pulses and a detailed finite-element method and cable model of the AN [5]). If a given pulse amplitude is above threshold, a spike is generated and threshold is elevated for a given time, to reflect the impact of refractoriness and spike-rate adaptation. Absolute refractoriness is 0.7 ms, followed by a 6-dB increase in threshold decreasing with a time constant of 1.5 ms.

JO17 model. We implemented a population-response version of the model developed by Joshi et al. [6]. 1500 neurons were created, with the input current for each neuron scaled to match the thresholds of the BR22 model. For each neuron, the model consists of two leaky integrate-and-fire elements, one that is anodic-sensitive and one that is cathodic-sensitive. By construction, the model shows effects of refractoriness, facilitation, spike-rate adaptation and accommodation. Time constants of facilitation (∼200 µs) and refractoriness (abs. 600 µs, rel. refractoriness tapering off within 4-5 ms) match those of recordings in cats.

Stimuli. We created two sets of stimuli, identical to the ones used in [4]. In the first set, two pulse trains with a carrier rate of 480 pps were modulated respectively at 80 Hz and 120 Hz. The IPI between both carrier rate was varied from 0 to ∼ 1 ms (maximum IPI given the carrier rate). In the second set, the NDR-generating stimulus was the same, albeit with a fixed IPI of 0 µs, and we additionally created a single pulse train modulated at 40 Hz, as we did in [4] to generate an auditory steady-state response (eASSR). In both cases stimulation levels were set to recruit ∼ 10 % of the neurons.

Data processing. Stimuli of 2-s duration were passed through each model, with the first second of the response ignored to remove the impact of onset effects. Neural responses were summed across all neurons, and passed through an FFT (1-s signal, providing a 1-Hz resolution). Amplitude at 40 Hz was extracted for each condition, with its significance assessed against the noise floor at neighboring bins with an F test.

[1] Both models included spike-rate adaptation, and the JO17 model included accommodation, but those phenomena did not contribute significantly to the NDR generation.

3. RESULTS

3.1 Effect of IPI

Figure 1 shows the simulated effects of changing the IPI between the two carrier rates on the strength of the NDR. There was no effect of IPI for the BR22 model, and a beating pattern for the JO17 model with a dip at 0 µs. Neither model recreated the tapering-off pattern seen in CI users. Changing the refractoriness time constant of the BR22 model to have 200 µs of absolute refractoriness and a time constant of 200 µs for the relative refractoriness did recreate the pattern seen in CI users.

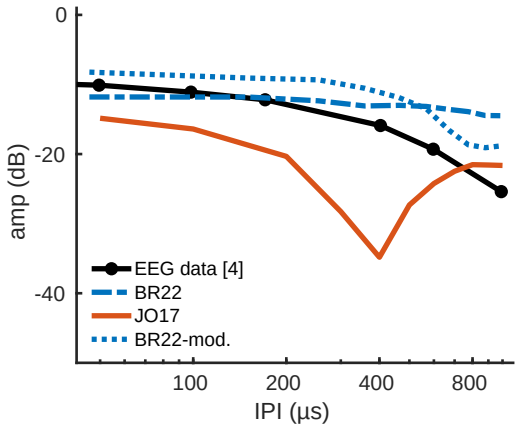

Figure 1. *Black, circles.* EEG data from [4]. *Red, solid.* Simulated NDR, JO17 model. *Blue, dashed.* Simulated NDR, BR22 model. *Blue, dotted.* Simulated NDR, modified BR22 model.

The underlying mechanism of NDR generation varied depending on the model and IPI. For the JO17 model and at short IPIs, facilitation between high-amplitude pulses increased neural response around the 22-ms mark (Fig. 2). Indeed, for the last F2 pulse in the cycle, 10.9% of the neurons spiked when both pulse trains were combined, instead of 4.7% when simulating each pulse train in isolation.

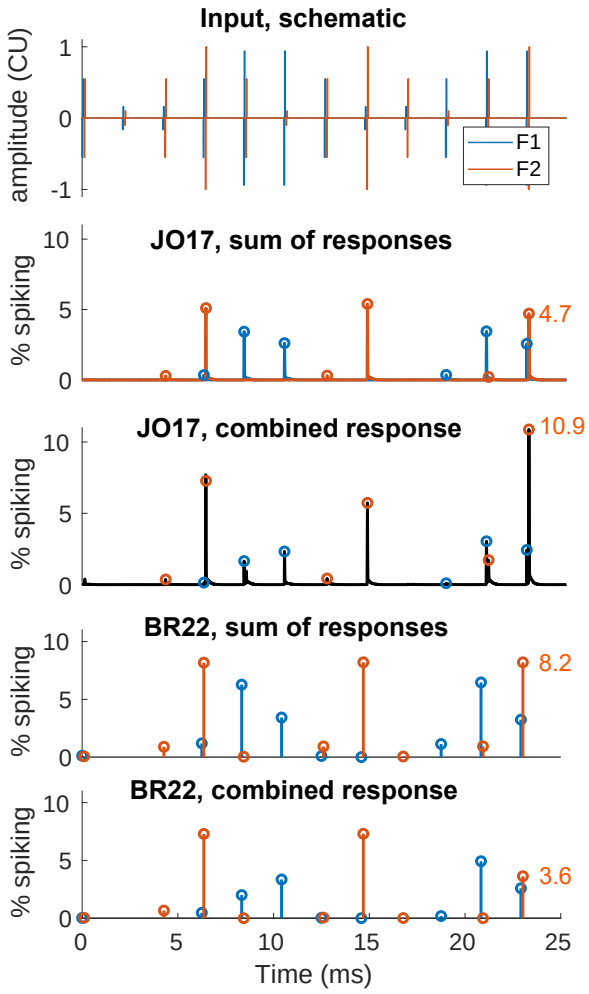

Figure 2. Averaged spiking within a single 40-Hz cycle. *Top.* Schematic, input (IPI = 8 µs). *Rows 2 and 3.* Output of JO17 model, when sum response to each pulse train (row 2) and when simulating the combined output (row 3). *Rows 4 and 5.* Same, but with the unmodified BR22 model. The red numbers show the peak value in response to the last F2 pulse of each cycle.

At IPIs above 400 µs in JO17, and all IPIs for the BR22 model, refractoriness caused a decreased neural response around the 22-ms mark (bottom panels of Fig. 2). For example, for the BR22 model, the response to the same last pulse of the F2 pulse train went down from 8.2% to 3.6% of all neurons. In both cases this creates a component at 40 Hz, but with a shift in phase of π between the two neural mechanisms. This explains the dip seen with the JO17 model in Figure 1, where both mechanisms contribute equally.

3.2 NDR phase comparison with measured data

We compared the phase of the NDR generated by each model with measured data in [4]. Because the neural generators of the EEG response are located in the thalamus/cortex, we need to take into account individual group delays in the response. We therefore re-referenced the NDR phase to the phase measured with the eASSR condition (obtained by stimulating with a single modulated pulse train), where we expect the strongest neural response to occur at the peak of the modulation cycle. Results are shown in Figure 3. For the four participants where we measured both eASSR and NDRs, the difference between the two phases was better predicted by the un-modified BR22 model (refractoriness-driven).

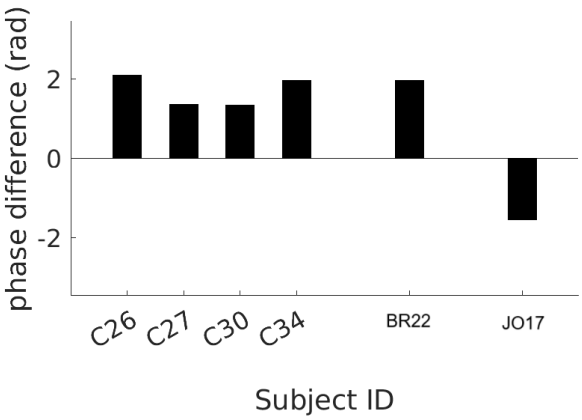

Figure 3. Measured phase difference between an NDR and eASSR at 40 Hz, for four CI users ([4]) and both models (unmodified BR22).

4. DISCUSSION

We investigated two phenomenological models of the AN, one that included refractoriness and spike-rate adaptation (BR22), and one that additionally included facilitation and accommodation (JO17). Both models created a distortion at 40 Hz. At IPIs below 400 µs and in the JO17 model, this was driven by facilitation between pulses, while at

IPIs above 400 µs (and all IPIs for the BR22 model), refractoriness was the main generation mechanism.

Neither model predicted the reduction in NDR at longer IPIs seen in humans, but a modified version (with a faster release from refractoriness) of the BR22 model could. The time constants of refractoriness had to be shortened significantly (200 µs of absolute refractoriness, time constant of 200 µs for the relative refractoriness) in order to match our results. This could suggest that refractoriness time constants of the AN are shorter than often assumed. However we did not model any other stages than the AN, and brainstem/thalamus/cortical stages also might contribute to a reduction of the NDR at long IPIs.

The phases of refractoriness-based and facilitation-based NDRs were predicted to be offset by a factor of π. When comparing to data measured in CI users [4], a better fit was obtained with refractoriness-based NDRs. This suggests that at comfortably loud levels, only a small proportion of neurons might show facilitative effects. For example, loudness perception at comfortably loud levels has been successfully modelled using only refractoriness and central integration [7].

Because it is difficult to measure AN response to high-rate pulse trains, a combination of modelling and EEG recordings such as presented here could be helpful in understanding which key mechanisms are at play in the perception of complex stimuli. The approach does not only suggest what types of interactions dominate the neural response, it also suggests that AN models may need to be modified to more accurately represent AN processing of sounds.

5. CONCLUSION

Distortions may already be present at the level of the AN and reflect core temporal-interaction mechanisms. Comparing computational modelling simulations to EEG data is promising for understanding how the AN processes the output of CIs.

6. REFERENCES

[1] F.-G. Zeng, S. Rebscher, W. Harrison, X. Sun, and H. Feng, "Cochlear implants: system design, integration, and evaluation.," *IEEE reviews in biomedical engineering*, vol. 1, pp. 115–42, 2008.

[2] J. Boulet, M. White, and I. C. Bruce, "Temporal Considerations for Stimulating Spiral Ganglion Neurons with Cochlear Implants," *Journal of the Association for Research in Otolaryngology*, vol. 17, no. 1, pp. 1–17, 2016.

[3] R. P. Carlyon, F. Guérit, J. M. Deeks, A. Harland, R. Gransier, J. Wouters, S. R. de Rijk, and M. Bance, "Using Interleaved Stimulation to Measure the Size and Selectivity of the Sustained Phase-Locked Neural Response to Cochlear Implant Stimulation," *Journal of the Association for Research in Otolaryngology*, vol. 22, no. 2, pp. 141–159, 2021.

[4] F. Guérit, J. M. Deeks, D. Arzounian, R. Gransier, J. Wouters, and R. P. Carlyon, "Using Interleaved Stimulation and EEG to Measure Temporal Smoothing and Growth of the Sustained Neural Response to Cochlear-Implant Stimulation," *Journal of the Association for Research in Otolaryngology*, vol. 24, no. 1, pp. 253–264, 2023.

[5] T. Brochier, J. Schlittenlacher, I. Roberts, T. Goehring, C. Jiang, D. Vickers, and M. Bance, "From Microphone to Phoneme: An End-to-End Computational Neural Model for Predicting Speech Perception With Cochlear Implants," *IEEE Transactions on Biomedical Engineering*, vol. 69, no. 11, pp. 3300–3312, 2022.

[6] S. N. Joshi, T. Dau, and B. Epp, "A Model of Electrically Stimulated Auditory Nerve Fiber Responses with Peripheral and Central Sites of Spike Generation," *Journal of the Association for Research in Otolaryngology*, vol. 18, no. 2, pp. 323–342, 2017.

[7] C. M. McKay, M. D. Remine, and H. J. McDermott, "Loudness summation for pulsatile electrical stimulation of the cochlea: effects of rate, electrode separation, level, and mode of stimulation.," *The Journal of the Acoustical Society of America*, vol. 110, no. 3 Pt 1, pp. 1514–1524, 2001.